Effect of Fiber Volume Fraction on the Stress Intensity Factors for Multi Layered Composites Under Arbitrary Anti-Plane Shear Loading

Sung Ho KIM
Manaufacturing Director in Varian Korea Limited
Kang Yong LEE*
Professor in Department of Mechanical Engineering, Yonsei University
Sung Chul JOO
Former Graduate Student in Department of Mechanical Engineering, Yonsei University
(Currently, Engineer in Korea Electric Co.)

A multi-layered orthotropic material with a center crack is subjected to an anti-plane shear loading. The problem is formulated as a mixed boundary value problem by using the Fourier integral transform method. This gives a Fredholm integral equation of the second kind. The integral equation is solved numerically and anti-plane shear stress intensity factors are analyzed in terms of the material orthotropy for each layer, number of layers, crack length to layer thickness and the order of the loading polynomial. Also, the case of monolithic and hybrid composites are investigated in terms of the local fiber volume fraction and the global fiber volume fraction.

Key Words : Stress Intensity Factor, Multi Layer, Auti-Plane Shear Loading

Nomenclature

a	: Half crack length
$A_j(\xi)$, $B_j(\xi)$	: Unknown coefficients
$g(x)$	: Arbitrary anti-plane shear crack surface loading
G_j	: Fourier transform function for the j_{th} layer
h_j	: Distance from the crack to the exterior interface of the j_{th} layer
$J_0(\xi t)$, $J_1(\xi t)$	: Bessel function of the first kind of order 0 and 1, respectively
n	: Number of layers
N_L and N_M	: Number of integration points for Gaussian Integration
K_{IIIL}, K_{IIIR}	: Mode III stress intensity factors for left and right hand side crack tips, respectively
p_{2k}, p_{2k+1}	: Influence coefficients for symmetric and anti-symmetric loading parts, respectively
q	: Order of each term of polynomial loading
t_{mo}	: Thickness of cracked matrix layer
t_f, t_m	: Thickness of fiber layer and matrix layer, respectively
V_{GF}	: Global Fiber volume fraction
V_{LF}	: Local Fiber volume fraction
W_k, W_m	: Integration constants for Gaussian Quadrature integration
β_j	: Directional modulus for the j_{th} layer $\left(\sqrt{\frac{\mu_{x(j)}}{\mu_{y(j)}}}\right)$
$\mu_{x(j)}$	: Shear modulus in x direction for the j_{th} layer

* Corresponding Author,
E-mail : fracture@yonsei.ac.kr
TEL : +82-2-361-2813 ; **FAX** : +82-2-312-2159
Department of Mechanical Engineering, Yonsei University, 134 Sinchon-Dong, Seodaemun-ku, Seoul 120-749, Korea.(Manuscript **Received** August 16, 1999; **Revised** June 5, 2000)

$\mu_{y(j)}$: Shear modulus in y direction for the j_{th} layer

ξ : Fourier transformation variable

$\tau_{yz(j)}$, $\tau_{xz(j)}$: Stress components for the j_{th} layer

τ_m, α_r : Integration abscissas for Gaussian_Quadrature integration

$w_{(j)}$: Displacement components in z direction for the j_{th} layer

1. Introduction

Layered materials can be used for high performance structures to have a high strength-to-weight ratio and, when cracks are present, there is the potential danger that they might cause premature failure. The intensity of the stress ahead of the crack tip is a parameter to evaluate how load, composite geometry and material would affect the local stress field. The critical value of the stress intensity factor is used to study the fracture behavior of layered composites. Sih and Chen(1981) used Integral transforms for studying composite materials with cracks under two- and three-dimensional loads. An interface crack between two different orthotropic layers under plane extension is studied by Zhang (1989) ; Sung and Liou(1995) studied the case of an internal crack in a clamped orthotropic half plane. Stress intensity factor using finite elements was calculated by Lengo and McCallion(1997) for orthotropic materials ; boundary integral was applied to solve the problem of crack normal to the multi-layered interface under tension(Lin and Keer, 1989). Anti-symmetric loading and combined normal and shear loads solved by Lee et al. (1994 ; 1996). An inter-laminar crack under normal and shear load in multi-layered materials were studied in previous studies(Kim et al. 1998a; 1998b).

The anti-plane shear stress intensity factor for a finite interface crack between inner layers of four-layered composite was examined by Chen and Sih (1973) and the case for anti-symmetric shear loadings was investigated by Erdogan and Gupta (1971). Three-layered orthotropic material with a crack under anti-plane shear loading was reported by Kim et al. (1999). This paper investigates the multi-layered orthotropic material with a crack under anti-plane shear loading. A Fredholm integral equation is derived by the Fourier integral transform method to evaluate the anti-plane shear stress intensity factor by solving the integral equation numerically. The effects of material orthotropy for each layers, number of layers, crack length to layer thickness and the order of the loading polynomial are evaluated. Also, the case of monolithic and hybrid composites are investigated in terms of the local fiber volume fraction and the global fiber volume fraction.

2. Problem Formulation

Consider a plane strain type multi-layered material with a center crack subjected to an anti-plane shear crack surface loading as illustrated in Fig. 1. The crack surface is parallel to the layer interface and perfect bonding between orthotropic layers is assumed. Using the Fourier integral transformation, stress and displacement components can be formulated as given by Kim et al. (1999).

$$\tau_{yz(j)}=\mu_{y(j)}\frac{2}{\pi}\int_0^\infty \frac{\partial G_j}{\partial y}\begin{bmatrix}\cos\xi x\\ \sin\xi x\end{bmatrix}d\xi$$

$$\tau_{xz(j)}=\mu_{x(j)}\frac{2}{\pi}\int_0^\infty G_j\xi\begin{bmatrix}-\sin\xi x\\ \cos\xi x\end{bmatrix}d\xi$$

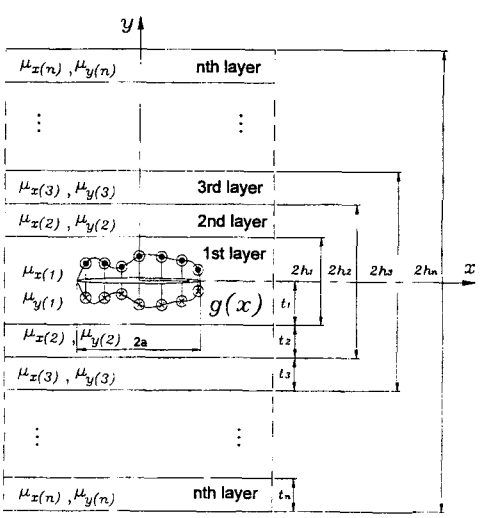

Fig. 1 Geometry and configuration of the model

$$w_{(j)}=\frac{2}{\pi}\int_0^\infty G_j\begin{bmatrix}\cos\xi x\\ \sin\xi x\end{bmatrix}d\xi \tag{1}$$

where $G_j(\xi, y)=A_j(\xi)e^{\xi_j y}+B_j(\xi)e^{-\xi_j y}$

and $\xi_j=\sqrt{\frac{\mu_{x(j)}}{\mu_{y(j)}}}\,\xi$ $(j=1, 2, 3, \cdots, n)$ (2)

The subscript j=1 represents the first layer where a crack is located and $\tau_{yz(j)}$, $\tau_{xz(j)}$ and $w_{(j)}$ represent stress and displacement components. $\mu_{x(j)}$ and $\mu_{y(j)}$ are x and y directional shear moduli of the j-th layer, and coefficients A_j and B_j are to be determined.

Referring to Fig. 1, only the upper half plane is considered due to the symmetry; boundary conditions are

$$\begin{aligned}
&\tau_{yz(1)}=-g(x) \quad |x|\le a,\ y=0\\
&w_{(1)}=0 \quad |x|>a,\ y=0\\
&\tau_{yz(j)}=\tau_{yz(j+1)} \quad |x|<\infty,\ y=h_j (j=1,\\
&\qquad \cdots, n-1)\\
&w_{(j)}=w_{(j+1)} \quad |x|<\infty,\ y=h_j (j=1,\\
&\qquad \cdots, n-1)\\
&\tau_{yz(n)}=0 \quad |x|<\infty,\ y=h_n
\end{aligned} \tag{3}$$

where $h_j (j=1, \cdots, n)$ is the interfacial location coordinate to j-th layer and $g(x)$ is an anti-plane shear crack surface loading.

$$\begin{aligned}
g(x)&=\sum_{q=0}^{\infty}p_q\left(\frac{x}{a}\right)^q\\
&=\sum_{k=0}^{\infty}p_{2k}\left(\frac{x}{a}\right)^{2k}+\sum_{k=0}^{\infty}p_{2k+1}\left(\frac{x}{a}\right)^{2k+1}
\end{aligned} \tag{4}$$

where p_{2k} and p_{2k+1} are the given influence coefficients for the symmetric and anti-symmetric loading parts, respectively.

The crack surface loading $g(x)$ is separated into symmetric and anti-symmetric loading parts without loss of generality. By applying the boundary conditions (3) to Eq. (1) , a pair of dual integral equations is obtained for each loading part as follows,

$$\int_0^\infty N(\xi)\begin{bmatrix}\cos\xi x\\ \sin\xi x\end{bmatrix}d\xi=\begin{bmatrix}0\\ 0\end{bmatrix} \quad |x|>a \tag{5}$$

$$\begin{aligned}
&\int_0^\infty \xi F(\xi)M(\xi)\begin{bmatrix}\cos\xi x\\ \sin\xi x\end{bmatrix}d\xi\\
&=\frac{\pi}{2\sqrt{\mu_{x(1)}\mu_{y(1)}}}\begin{pmatrix}p_{2k}\left(\frac{x}{a}\right)^{2k}\\ p_{2k+1}\left(\frac{x}{a}\right)^{2k+1}\end{pmatrix} \quad |x|\le a
\end{aligned} \tag{6}$$

where

$$F(\xi)\equiv-\frac{A_1(\xi)-B_1(\xi)}{M(\xi)} \tag{7}$$

$$M(\xi)\equiv A_1(\xi)+B_1(\xi) \tag{8}$$

Furthermore, $A_1(\xi)$ and $B_1(\xi)$ are defined as follows :

$$T=Q^{-1}R \tag{9}$$

where

$$T=[B_1, A_2, B_2, A_3, B_3, \cdots, A_n, B_n]^T \tag{10}$$

$$R=[R_1, R_2, R_3, \cdots, R_{2n-1}]^T \tag{11}$$

$$R_1=\Gamma_1\times e^{\beta_1\frac{H_1}{a}\tau}\times A_1(\xi),\ R_2=e^{\beta_1\frac{H_1}{a}\tau}\times A_1(\xi)$$

$$R_3=R_4=\cdots=R_{2n-1}=0\ (\Gamma_1\equiv\sqrt{\mu_{x(1)}\mu_{y(1)}}\ /\ \sqrt{\mu_{x(2)}\mu_{y(2)}},\ \beta_1\equiv\sqrt{\mu_{x(1)}/\mu_{y(1)}})$$

$$\bar{\xi}=a\xi,\ \Gamma_2\equiv\sqrt{\mu_{x(2)}\mu_{y(2)}}\ /\ \sqrt{\mu_{x(3)}\mu_{y(3)}}$$

where, Γ_1 indicates the ratio of strength of cracked layer and the neighboring layer while β_1 denotes the degree of orthotropy for the cracked layer and Q is found in Appendix.

By following the method by Copson(1961),

$$M(\xi)=\int_0^a\begin{bmatrix}\phi_{2k}(t)J_0(\xi t)\\ \phi_{2k+1}(t)J_1(\xi t)\end{bmatrix}dt \tag{12}$$

where J_0 and J_1 are the Bessel functions of the first kind of order 0 and 1, respectively. Also, $\phi_{2k}(t)$ and $\phi_{2k+1}(t)$ are to be determined. By Eq. (12), Eq. (5) is satisfied automatically and Eq. (6) is reduced to the form of Fredholm integral equation of a second kind.

$$\begin{aligned}
&\begin{bmatrix}\Phi_{2k}(\sigma)\\ \Psi_{2k+1}(\sigma)\end{bmatrix}+\int_0^1 K(\tau, \sigma)\begin{bmatrix}\Phi_{2k}(\tau)\\ \Psi_{2k+1}(\tau)\end{bmatrix}d\tau\\
&=\begin{bmatrix}q_{2k}(\sigma)\\ f_{2k+1}(\sigma)\end{bmatrix}
\end{aligned} \tag{13}$$

where

$$K(\tau, \sigma)\equiv\sqrt{\tau}\sqrt{\sigma}\int_0^\infty \alpha(F(\alpha/a)-1)\begin{bmatrix}J_0(\alpha\tau)J_0(\alpha\sigma)\\ J_1(\alpha\tau)J_1(\alpha\sigma)\end{bmatrix}d\alpha$$

$$q_{2k}(\sigma)=\frac{(2k-1)!!}{(2k)!!}\sigma^{2k+1/2}$$

$$f_{2k+1}(\sigma)=\frac{(2k+1)!!}{(2k+2)!!}\sigma^{2k+3/2}$$

$$(2k+2)!!=(2k+2)\times(2k),\ \cdots,\ 4\times2$$

$$(2k+1)!!=(2k+1)\times(2k-1),\ \cdots,\ 3\times1$$

$$(2k)!!=(2k)\times(2k-2),\ \cdots,\ 4\times2$$

$$(2k-1)!!=(2k-1)\times(2k-3),\ \cdots,\ 3\times1$$

$$t \equiv a\tau,\ s \equiv a\sigma,\ \xi \equiv \frac{\alpha}{a},\ x \equiv a\bar{x}$$

$$\phi_{2k}(t) \equiv \frac{\pi p_{2k}}{2\sqrt{\mu_{x(1)}\mu_{y(1)}}} a\sqrt{\tau}\, \Phi_{2k}(\tau),\ \psi_{2k+1}(t) \equiv \frac{\pi p_{2k+1}}{2\sqrt{\mu_{x(1)}\mu_{y(1)}}} a\sqrt{\tau}\, \Psi_{2k+1}(\tau) \quad (14)$$

To solve the Fredholm integral equation, the Gaussian quadrature integration technique is utilized.

$$\begin{bmatrix} \Phi_{2k}(\sigma_n) \\ \Psi_{2k+1}(\sigma_n) \end{bmatrix} + \sum_{m=1}^{N_L} \begin{bmatrix} \Phi_{2k}(\tau_m) \\ \Psi_{2k+1}(\tau_m) \end{bmatrix} K(\tau_m, \sigma_n) W(\tau_m) = \begin{bmatrix} q_{2k}(\sigma_n) \\ f_{2k+1}(\sigma_n) \end{bmatrix} \quad (15)$$
$$(n=1, 2, \cdots, N_L)$$

where

$$K(\tau_m, \sigma_n) \equiv \sqrt{\tau_m \sigma_n} \sum_{r=1}^{N_M} \alpha_r \left[F(\alpha_r / a) - 1 \right] \begin{bmatrix} J_0(\alpha_r\tau_m) J_0(\alpha_r\sigma_n) \\ J_1(\alpha_r\tau_m) J_1(\alpha_r\sigma_n) \end{bmatrix} W(\alpha_r) \quad (16)$$

At $\sigma_n = \tau_n (n=1, 2, \cdots, N_L)$, $\Phi_{2k}(\tau_m)$ and $\Psi_{2k+1}(\tau_m)$ are determined numerically as follows,

$$\sum_{m=1}^{N_L} [\delta_{mn} + K(\tau_m, \tau_n) W(\tau_m)] \begin{bmatrix} \Phi_{2k}(\tau_m) \\ \Psi_{2k+1}(\tau_m) \end{bmatrix} = \begin{bmatrix} q_{2k}(\tau_n) \\ f_{2k+1}(\tau_n) \end{bmatrix} \quad (17)$$
$$(n=1, 2, \cdots, N_L)$$

$$K(\tau_m, \tau_n) \equiv \sqrt{\tau_m \tau_n} \sum_{r=1}^{N_M} \alpha_r \left[F(\alpha_r / a) - 1 \right] \begin{bmatrix} J_0(\alpha_r\tau_m) J_0(\alpha_r\tau_n) \\ J_1(\alpha_r\tau_m) J_1(\alpha_r\tau_n) \end{bmatrix} W(\alpha_r) \quad (18)$$

δ_{mn} is Kronecker's delta; $W(\tau_m)$ and $W(\alpha_r)$ are the weight factors for Gaussian quadrature with N_L and N_M being the number of integration points.

The stress intensity factors at the crack tips are calculated.

$$K_{IIIR} = \lim_{x \to a^+} \sqrt{2(x-a)\pi}\ \tau_{yz(1)}(x, 0)$$
$$K_{IIIL} = \lim_{x \to -a^-} \sqrt{-2(x+a)\pi}\ \tau_{yz(1)}(x, 0) \quad (19)$$

where K_{IIIR} and K_{IIIL} refer to the right and left crack tips, respectively. After some integral manipulation for $\tau_{yz(1)}(x, 0)$, it is found that

$$K_{IIIR} = \sqrt{\pi a} \sum_{k=0}^{\infty} \{\Phi_{2k}(1)\, p_{2k} + \Psi_{2k+1}(1)\, p_{2k+1}\}$$

$$K_{IIIL} = \sqrt{\pi a} \sum_{k=0}^{\infty} \{-\Phi_{2k}(1)\, p_{2k} + \Psi_{2k+1}(1)\, p_{2k+1}\} \quad (20)$$

3. Numerical Results and Discussion

Consider the case of orthotropic three-layered material (n=3) with two outer half spaces. The dimensionless stress intensity factors of the right crack tip, $K_{III} / p_0\sqrt{\pi a}$, is shown in Fig. 2 as a function of h_1 / a with $\Gamma=5.0$ and agrees with Chen and Sih(1973). The convergency of the numerical solution is listed in Table 1 and good accuracy is found.

Next, the case of multi-layer is considered. For simplicity, it is assumed that all the layers are composed of identical thickness ($t_1 = t_2 = \cdots = t_n = t_0$) and the values of the shear moduli of the layers are gradually increasing or decreasing. In Fig. 3, the dimensionless stress intensity factors for each term of polynomial loading increases as a / t_0 and shear modulus ratio increases. Also, the dimensionless stress intensity factors decreases as q increases as discussed in previous studies (Lee et al. 1994, 1996 ; Kim et al., 1998a, 1998b). When the layer is relatively thin ($a / t_0 = 4.0$), the dimensionless stress intensity factors decreases drastically as the number of layers (n) increases.

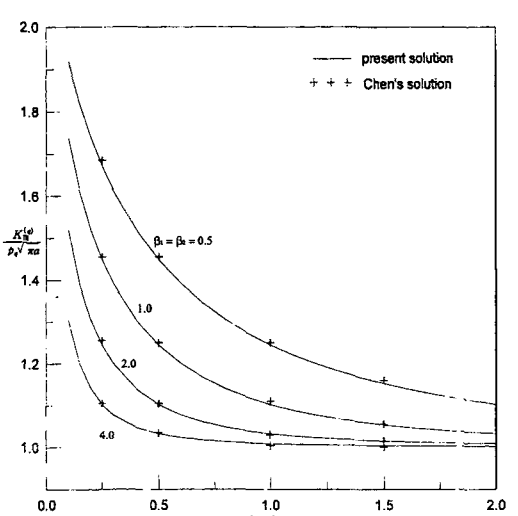

Fig. 2 Comparison of present numerical results with previous solution (Chen, 1973) with $\Gamma_1=5.0$ when $q=0$

Table 1 Converging behavior for dimensionless mode III SIFs for various numbers of Gaussian_Quadrature points.

		Dimensionless SIFs, $K_{III}/\tau_0\sqrt{\pi a}$			
		$\Gamma=2.0$	$\Gamma=2.0$	$\Gamma=0.5$	$\Gamma=1.0$
		$\beta_1=1.0$	$\beta_1=1.0$	$\beta_1=2.0$	$\beta_1=0.5$
		$\beta_1=1.0$	$\beta_2=1.0$	$\beta_2=2.0$	$\beta_2=0.5$
		$a/h_1=1.0$	$a/h_1=1.0$	$a/h_1=3.0$	$a/h_1=5.0$
N_G	N_Q	$a/h_2=0.5$	$a/h_2=0.1$	$a/h_2=0.5$	$a/h_2=0.5$
48	20	1.0856469	1.0540672	0.9230966	1.1493117
	30	1.0856469	1.0540672	0.9230966	1.1493117
	50	1.0856469	1.0540672	0.9230966	1.1493117
	100	1.0856469	1.0540672	0.9230966	1.1493117
54	20	1.0856474	1.0540673	0.9230966	1.1493118
	30	1.0856474	1.0540673	0.9230966	1.1493118
	50	1.0856474	1.0540673	0.9230966	1.1493118
	100	1.0856474	1.0540673	0.9230966	1.1493118
60	20	1.0856471	1.0540673	0.9230967	1.1493119
	30	1.0856471	1.0540673	0.9230967	1.1493119
	50	1.0856471	1.0540673	0.9230967	1.1493119
	100	1.0856471	1.0540673	0.9230967	1.1493119

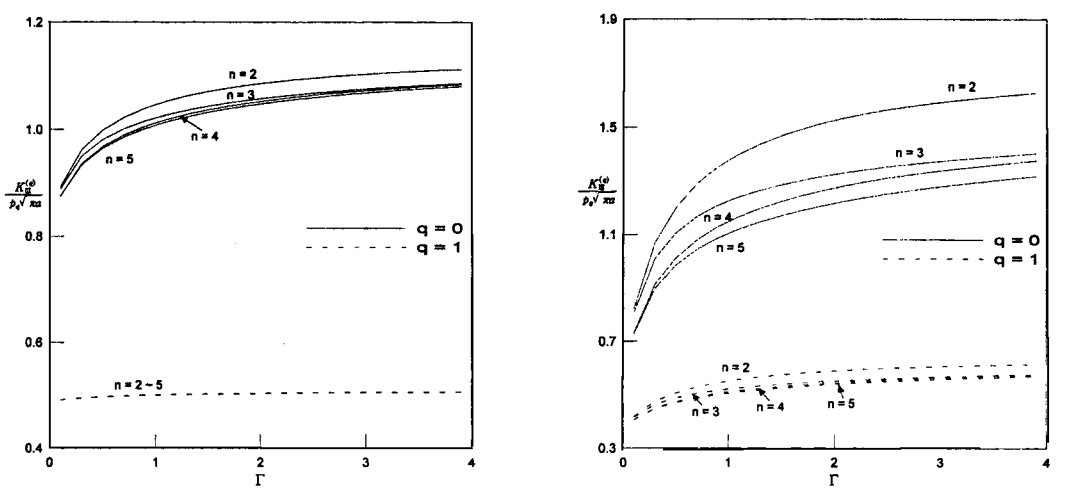

(a) $a/t_0=1.0$ (b) $a/t_0=4.0$

Fig. 3 Dimensionless mode III stress intensity factor for multi-layer case: (a) $a/t_0=1.0$ and (b) $a/t_0=4.0$

3.1 Case of monolithic composites

As an application of the multi-layered analysis, the case of monolithic composites composed of E-glass and epoxy is considered in Fig. 4. The material properties are summarized in Table 2. The local fiber volume fraction near the cracked epoxy layer region, V_{LF}, is defined as

$$V_{LF}=\frac{t_f}{t_{mo}+t_f} \tag{21}$$

Also, the global fiber volume fraction far from the cracked epoxy layer region, V_{GF}, is defined as

$$V_{GF}=\frac{t_f}{t_m+t_f} \tag{22}$$

In the numerical analysis, V_{LF} was selected to be equal to 0.2 and 0.8, whereas V_{GF} was the values 0.3, 0.5 and 0.8 and a/t_{mo} varing from 0.1 to 2. 0. In Fig. 5, the dimensionless stress intensity

Table 2 The material properties used for composites (Schwartz, 1992)

Type	Shear modulus (GPa)	
	μ_x	μ_y
E-glass	35.0	7.0
Boron	165.0	28.0
Epoxy	1.33	1.33

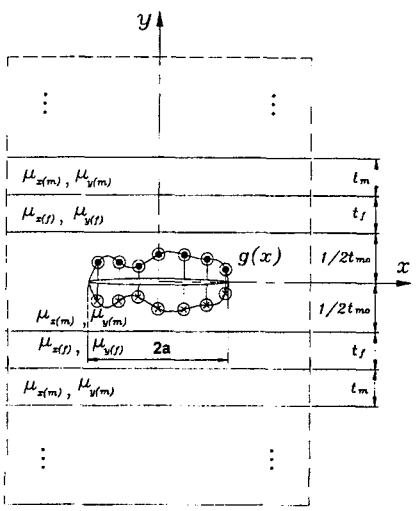

Fig. 4 Geometry of monolithic composites

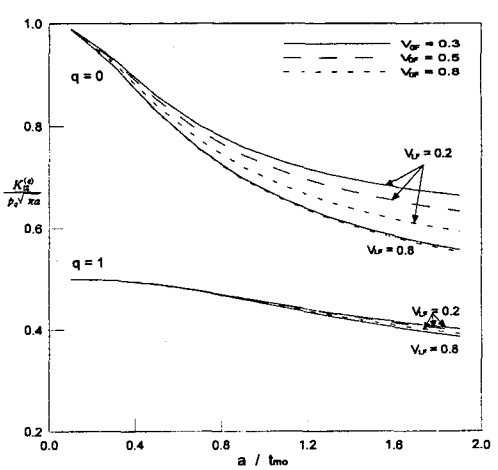

Fig. 5 Dimensionless mode III stress intensity factor for monolithic composites

factors for each term ($q=0$ and 1) of polynomial loading and for various local and global fiber volume fractions are analyzed. When the local fiber volume fraction is high ($V_{LF}=0.8$), the global fiber volume fraction does merely influence the stress intensity factors. When the local fiber volume fraction is low ($V_{LF}=0.2$), however, the global fiber volume fraction (V_{GF}) contributes significantly to the dimensionless stress intensity factors if the cracked epoxy layer is thin ($a / t_{mo}>1$).

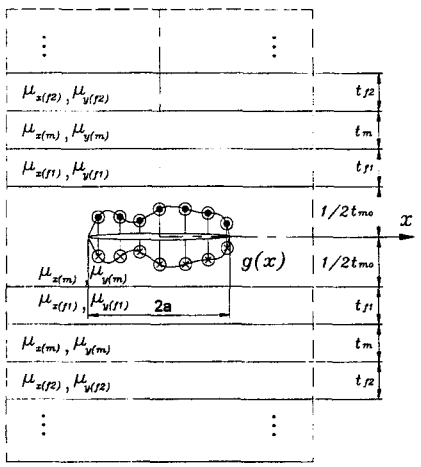

Fig. 6 Geometry of hybrid composites

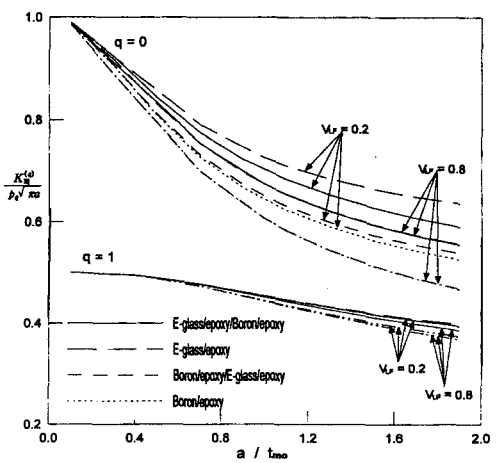

Fig. 7 Comparison of dimensionless mode III stress intensity factors between monolithic and hybrid composites

3.2 Case of hybrid composites

The hybrid composites case as shown in Fig. 6 is considered. The local fiber volume fraction near the cracked epoxy layer region, V_{LF}, is defined as

$$V_{LF}=\frac{t_{f_1}}{t_{mo}+t_{f_1}} \tag{23}$$

Also, the global fiber volume fraction far from the cracked epoxy layer region, V_{GF}, is defined as

$$V_{GF}=\frac{t_{f_1}+t_{f_2}}{2t_m+t_{f_1}+t_{f_2}} \tag{24}$$

In Fig. 7, the dimensionless stress intensity factors for each term of polynomial loading in case of various composites. The Boron-epoxy composites yields the smallest stress intensity factors.

4. Conclusions

The stresss intensity factors for a center crack subjected to an anti-plane shear loading in the orthotropic multi-layered material is analyzed by Fourier integral transform method. The following conclusions are obtained:

(1) The limiting case for the present solution agrees with Chen and Sih(1973).

(2) For the case of multi-layered material, the dimensionless stress intensity factors for each term of polynomial loading increases as crack length to layer thickness ratio and shear modulus ratio increases, and as the number of layer and the order of each term of polynomial loading decreases.

(3) For the case of monolithic and hybrid composites, it is found that relatively larger dimensionless stress intensity factors are produced when the local fiber volume fraction is low. Also, the global fiber volume fraction contributes significantly to the dimensionless stress intensity factors if the cracked matrix layer is thin.

Acknowledgements

The authors are grateful for the support provided by Brain Korea 21 from the Korea Research Foundation(KRF) and a grant from the Korea Science & Engineering Foundation(KOSEF) and Safety and Structural Integrity Research Center at the Sungkyunkwan University.

References

Bechel, V. T. and Kaw, A. K., 1994, "Fracture Mechanics of Composites with Nonhomogeneous Interphases and Nondilute Fiber Volume Fractions," *International Journal of Solids and Structures*, Vol. 31, No. 15, pp. 2053~2070.

Chen, E. P. and Sih, G. C., 1973, "Torsional and Anti-Plane Strain Delamination of an Orthotropic Layered Composite," *Proceedings of the 13th Midwestern Mechanics Conference*, Vol. 7, pp. 763~776.

Copson, E. T., 1961, "On certain dual integral equations," *Proceedings of the Glasgow Mathematical Association*, Vol. 5, pp. 19~24.

Erdogan, F. and Gupta, G., 1971, "The Stress Analysis of Multi-layered Composites with a Flaw," *International Journal of Solids and Structures*, Vol. 7, pp. 39~61.

Kim, S. H., Lee, K. Y. and Park, M. B., 1998a, "Mode II Stress intensity factors for inter-laminar cracked composites under arbitrary shear crack surface loading," *Engineering Fracture Mechanics*, Vol. 59, No. 4, pp. 509~520.

Kim, S. H., Lee, K. Y. and Park, M. B., 1998b, "Stress Intensity Factors for Inter-Laminar Cracked Composites Under Arbitrary Normal Crack Surface Loading," *International Journal of Solids and Structures*, Vol. 35, No. 33, pp. 4355~4367.

Kim, S. H., Lee, K. Y. and Joo, S. C., 1999, "Mode III Stress Intensity Factor for Orthotropic Three-Layered Material Under Arbitrary Anti-Plane Shear Loading," *Theoretical and Applied Fracture Mechanics*, in Press.

Lee., K. Y., Kim, S. H. and Park, M. B., 1994, "Stress Intensity Factors for Multi-Layered Material Under Anti-Symmetric Polynomial Loading," *Transactions of the Korean Society of Mechanical Engineers*, Vol. 18, pp. 3219~3226.

Lee, K. Y., Park, M. B. and Kim, S. H., 1996, "Stress Intensity Factors for Center Cracked Laminated Composites Under Arbitrary Crack Surface Loadings," *Trans. Korean Society of Mechanical Engineers*, Vol. 20, pp. 901~909.

Lengoc, L. and McCallion, H., 1997, "On the Fracture Toughness of Orthotropic Materials," *Engineering Fracture Mechanics*, Vol. 58, pp. 355~362.

Lin, W. and Keer, L. M., 1989, "Analysis of a

Vertical Crack in a Multi-layered Medium," *ASME Journal of Applied Mechanics*, Vol. 56, pp. 63~69.

Schwartz, M. M., 1992. Composite Materials Handbook, 2nd ed., McGraw Hill Inc.

Sih, G. C. and Chen, E. P., 1981, *Cracks in Composite Materials, Mechanics of Fracture*, Martinus Nijhoff Publishers, Vol. 6.

Sung, J. C. and Liou, J. Y., 1995, "Internal Crack in a Half-Plane Solid with Clamped Boundary," *Computer Methods in Applied Mechanics and Engineering*, Vol. 121, pp. 361~372.

Zhang, X. S., 1989, "Central Crack at the Interface Between Two Different Orthotropic Media for the Mode I and Mode II," *Engineering Fracture Mechanics*, Vol. 33, pp. 327~333.

Appendix

The elements of Q in Eq. (9) is as follows.

$$Q_{(2j-1)(2j-1)}=\Gamma_j e^{-\beta_j \frac{h_j\sqrt{-}}{a}\xi}$$

$$Q_{(2j-1)(2j)}=e^{\beta_{j+1}\frac{h_j\sqrt{-}}{a}\xi}$$

$$Q_{(2j-1)(2j+1)}=-e^{-\beta_{j+1}\frac{h_j\sqrt{-}}{a}\xi}$$

$$Q_{(2j)(2j-1)}=-e^{-\beta_j\frac{h_j\sqrt{-}}{a}\xi}$$

$$Q_{(2j)(2j)}=e^{\beta_{j+1}\frac{h_j\sqrt{-}}{a}\xi}$$

$$Q_{(2j)(2j+1)}=e^{-\beta_{j+1}\frac{h_j\sqrt{-}}{a}\xi}(j=1 \text{ to } n-1) \quad (A1)$$

$$Q_{(2j-1)(2j-2)}=-\Gamma_j e^{\beta_j\frac{h_j\sqrt{-}}{a}\xi}$$

$$Q_{(2j)(2j-2)}=-e^{\beta_j\frac{h_j\sqrt{-}}{a}\xi}(j=2 \text{ to } n-1) \quad (A2)$$

$$Q_{(2n-1)(2n-2)}=1.0$$

$$Q_{(2n-1)(2n-2)}=-e^{-2B_n\frac{h_n\sqrt{-}}{a}\xi} \quad (A3)$$

where $\beta_i=\sqrt{\mu_{x(i)}/\mu_{y(i)}}$, $\Gamma_j\equiv\sqrt{\mu_{x(j)}\mu_{y(j)}}\,/\,\sqrt{\mu_{x(j+1)}\mu_{y(j+1)}}$ $(j=1, \cdots, n-1)$

All other components are zero.